Regular Article

Detection of baby food sterilized with ionizing radiation using thermoluminescence

N. A. Kazakis[a] and Ch. Betsou

Laboratory of Archaeometry and Physicochemical Measurements, Athena-Research and Innovation Center in Information, Communication and Knowledge Technologies, Kimmeria University Campus, PO Box 159, 67100 Xanthi, Greece

Abstract Food sterilization with ionizing radiation is a well-established technology, which is constantly extending to several products due to its numerous advantages. However, radiosterilization is prohibited to several food categories, such as baby food products since it could cause nutrient degradation of such foods with significant effects on the infants' health. As a result, any governmental agency responsible for the detection of irradiated products should first focus on products consumed by babies/children. To this respect, the present work explores whether TL can be employed as a method for post-sterilization dosimetry on baby food, by studying the properties of their glass containers since they would be equally and jointly exposed to the ionizing radiation during the sterilization process. Two different reputable brands, i.e., Hipp® and Nestle®, are used for this purpose. Both glass containers exhibit a linear TL dose response for doses up to 3 kGy, while no sensitization of the main peaks is observed. Though their behavior is not very stable with time (strong fading) yet fading correction is possible. Dose recovery tests were successfully conducted, calculating the administered dose with high accuracy. A computerized curve deconvolution analysis (CCDA) was also performed revealing that all glow curves can be fitted with one peak of continuous trap distribution and three discrete-energy peaks, which also demonstrate a linear dose response over the range 50–3000 Gy. Thus, findings are very promising towards the post-sterilization dosimetry of baby food through their glass containers.

1 Introduction

Radiosterilization, namely the use of ionizing radiation (gamma radiation, electron beams or X-rays) is being applied in more than 40 countries worldwide for the sterilization of food and drugs, while such irradiated products are commercially available in more than 28 countries. Approved facilities for the treatment of food and/or food ingredients with ionizing radiation exist in 14 out of the 28 Member States of the European Union [1] where a significant number of food products (e.g. fruit, meats, poultry, spices) are authorized for radiosterilization in the EU [2]. Moreover, the Member States may not prohibit, restrict or hinder the marketing of foodstuffs irradiated as dictated by the EU Directive resulting in the free trade of such foodstuffs among the Member States of the EU. In addition, according to Directive 1999/2/EC [3] a foodstuff treated with ionizing radiation can also be imported from a third country if it has been treated in an irradiation facility approved by the European Community and complies with the conditions which apply to those foodstuffs. Based on the above, it is evident that irradiated food is in abundance and available in the European market.

However, when radiation passes through materials (e.g. food) it breaks chemical bonds and can initiate chemical reactions (e.g. formation of free radicals) causing degradation (e.g. activity, nutrition, odor, color, flavor, pH). Furthermore, food is introduced in the human body and interact with it with various ways. For example, the free radicals may harm cells including DNA, proteins, cell membranes, which may play a role in the development of malignancies or other health conditions [4]. Thus, it is not possible to know a priori if and how the free radicals produced at irradiated products interact with the consumer's body. A recent work [5] highlights that several animal studies demonstrated that consumption of irradiated food provoked genome instability raising serious concerns regarding oncogenic potential of irradiated consumables. Thus, all the above changes and the induced radiolysis may result in a toxicological hazard and put at risk the consumer's health.

All irradiated products in EU or those containing irradiated ingredients must carry the internationally accepted radiation symbol "radura", along with the

ᵃ e-mail: nikkazak@athenarc.gr (corresponding author)

words "irradiated" or "treated with ionizing radiation" [3], which however manufacturers may not comply with it. Moreover, in some countries the manufacturer is required to provide further proof regarding the potential degradation and safety of irradiated products. In addition, no information about the dose applied is given. The above, in conjunction with the fact that the food irradiation policies vary from country to country and that radiosterilization is permitted in some countries and not in others [6] leads to the necessity for methods to detect irradiated samples. Consequently, development of food irradiation detection methods, useful for regulatory compliance purposes, is an active area of investigation.

Several food products legally irradiated in many countries are probably also exported into countries that do not permit irradiation of any food. Therefore, all countries must have in place analytical methods to determine whether food has been irradiated or not [7] according to the EU legislation. The EU has certified few methods (e.g. Thermoluminescence-TL, Electron Spin Resonance-ESR) and issued European Standards which can be used for the detection of irradiated foods, but they have been validated only for specific food categories. Additionally, there is an extensive research work in the literature for the identification of irradiated food with the above methods, such as spices, herbs, fruits, meat etc.

However, it must be noted that detection of irradiated foods should also be conducted in a regular basis for certain products which are not included in the EU list of foods allowed to be treated with ionizing radiation and especially for those where radiosterilization is definitely prohibited, such as baby food products (as clearly stated by the Food and Agriculture Organization of the United Nations and the World Health Organization) [8]. Infants/children constitute a sensitive population from many points of view. They are growing and developing, thus differ from adults in composition/metabolism as well as in physiological/biochemical processes [9]. Several researchers support that the nutrient degradation (e.g. vitamin, protein loss) of foods caused by irradiation is not considerable in the overall diet [10], since the proportion of the irradiated food in diet may be relatively low, but this is not true for infants, since such products is their exclusive food source for a long time. Thus, minor nutrient degradation of such foods can have significant effects on the infants' health. As a result, any governmental agency responsible for the detection of irradiated products should first focus on products consumed by babies/children.

Based on the literature, there are no studies exploring the possibility to identify any kind of irradiated baby food using any of the above methods. There is no work aiming at the development of a TL/OSL protocol according to the EU standards describing the complete procedure for the detection of irradiated baby food. Based on the above, the scope of the present work is to explore the possibility to identify/detect and assess the dose (if possible) of irradiated baby foods

Fig. 1 Images of the baby food products whose glass containers were studied: **a** Hipp and **b** Nestle

with Thermoluminescence (TL), for upholding regulatory controls, checking compliance against labelling requirements, facilitating international trade and reinforcing consumer confidence.

The above is achieved in the present study through the thorough investigation of the luminescence (TL) properties of the glass containers of specific baby foods since they would be equally and jointly exposed to the ionizing radiation during the sterilization process. A computerized curve deconvolution analysis (CCDA) of the TL signals for doses up to 3 kGy is also conducted to gain an insight into the trap properties and signal time-stability of the glass containers.

2 Experimental procedure

2.1 Food selection and sample preparation

Commercial baby food of two different brands (Hipp® and Nestle®) were selected for the present study. The above brands were also selected based on their "reputation" and availability in the market ensuring their widespread availability in stores and houses all over the world, and thus enhancing the applicability range of the findings for other purposes as well (e.g. retrospective/accidental dosimetry).

The products (Fig. 1) were supplied from a supermarket sealed and before their expiration date as suggested by the manufacturer. Please note, from here on, unless otherwise stated, the terms "Hipp" and "Nestle" refer to the respective glass containers rather than the food substance.

2.2 Sample preparation

The same procedure with Kazakis et al. [11] was followed for the cleaning of the glass containers and the preparation of the samples. In short, the glass containers were soaked in distilled water to remove the labels and the glue underneath. The containers were then
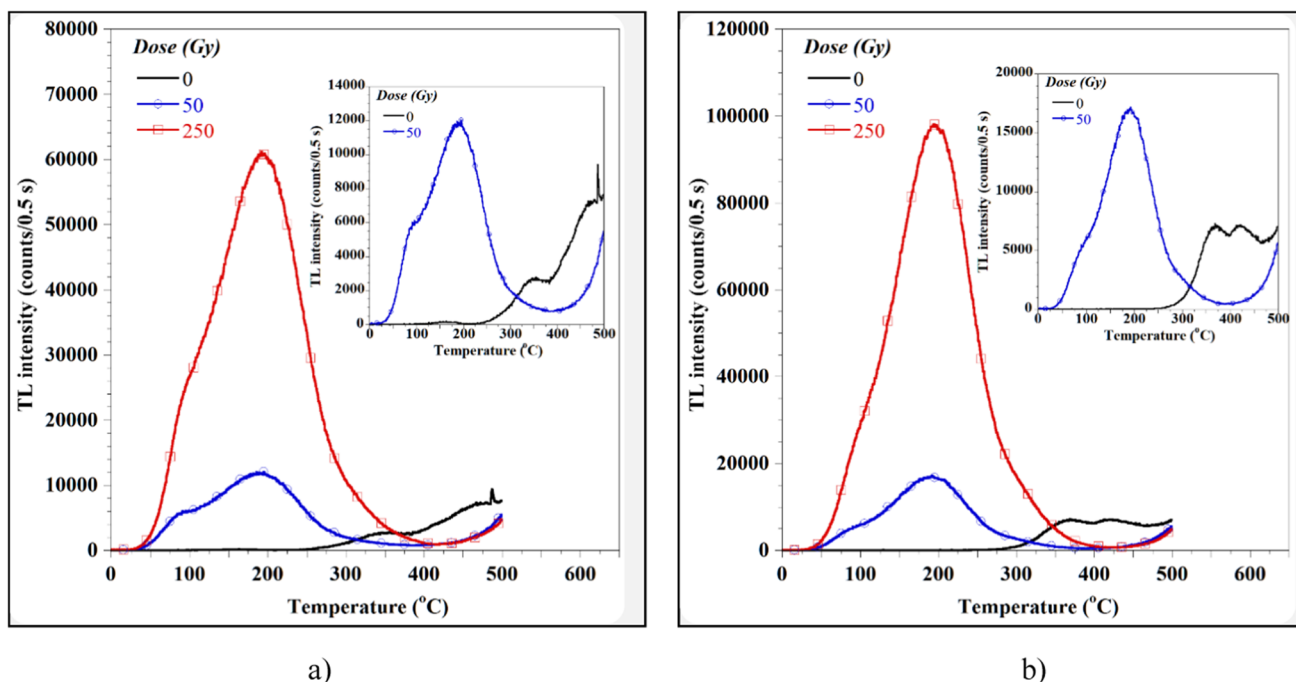
a)

b)

Fig. 2 Typical TL glow curves for both glass containers: **a** Hipp and **b** Nestle. The insets illustrate magnification of the glow curve after a dose of 50 Gy along with the zero-dose glow curve; markers are used for illustration purposes

washed under running distilled water to completely discard any remains to assure that no contribution to the acquired signal would be made by the label material and/or the glue.

In the same respect, after disposing of the food from all containers, the latter were first thoroughly cleaned using running distilled water. Then, the containers were further cleaned in an ultrasonic bath to completely remove any food remains in their interior and/or contamination at their exterior part. No chemical or thermal treatment was employed for the cleaning of the glass containers to avoid any undesired spurious signal.

Finally, the dried glass containers were gently crashed and ground in a mortar to produce small glass particles. The latter were further sieved and glass grains of size 75–150 μm were selected for the TL measurements.

2.3 Instruments and methods

A Riso TL/OSL reader (model TL/OSL-DA-15) was used for the TL measurements, equipped with a ^{90}Sr/^{90}Y beta particle source. The detection system consists of a photomultiplier tube and the combination of two filters: a Corning 7–59 (320–480 nm) and a heat absorbing Pilkington HA-3 filter. All TL measurements were performed in a nitrogen atmosphere with a low constant heating rate of 2 °C/s up to a maximum temperature of 500 °C/s.

Beta-doses from 50 up to 3000 Gy were applied in aliquots of about 8.5 mg, while several measurements were conducted in two different samples for each glass container, in order to ensure the repeatability of the results. The above dose range was selected to explore

the suitability of the glass containers in all possible dosimetric uses (accidental and post-sterilization).

3 Results and discussion

3.1 TL glow curve

Figure 2 illustrates typical glow curves for both glass containers. The shape of the glow curves is similar for both containers, namely they consist of at least three overlapping peaks: one centered at low temperatures (~ 90–100 °C), one broader at ~ 190–200 °C and a smaller one at a higher temperature, i.e., ~ 280–300 °C. As the dose increases the peaks tend to merge into a single peak of broad FWHM. This is indicative of the amorphous state of the glasses. Similar glow curves have also been observed by other investigators who studied the TL properties of various types of glasses [11–14]. In amorphous materials the trap depths associated with particular defects are spread over a range of values rather than being uniquely defined resulting in distributed activation energies rather than discrete [15].

A zero-dose (natural) signal is also present at temperatures > 260–280 °C. The source of this signal is unknown. This inherent signal overlaps with the tail of the curve after a dose has been applied. Yet, this is not a drawback if the signal of temperatures below the above threshold can be used for dosimetry purposes (see below).
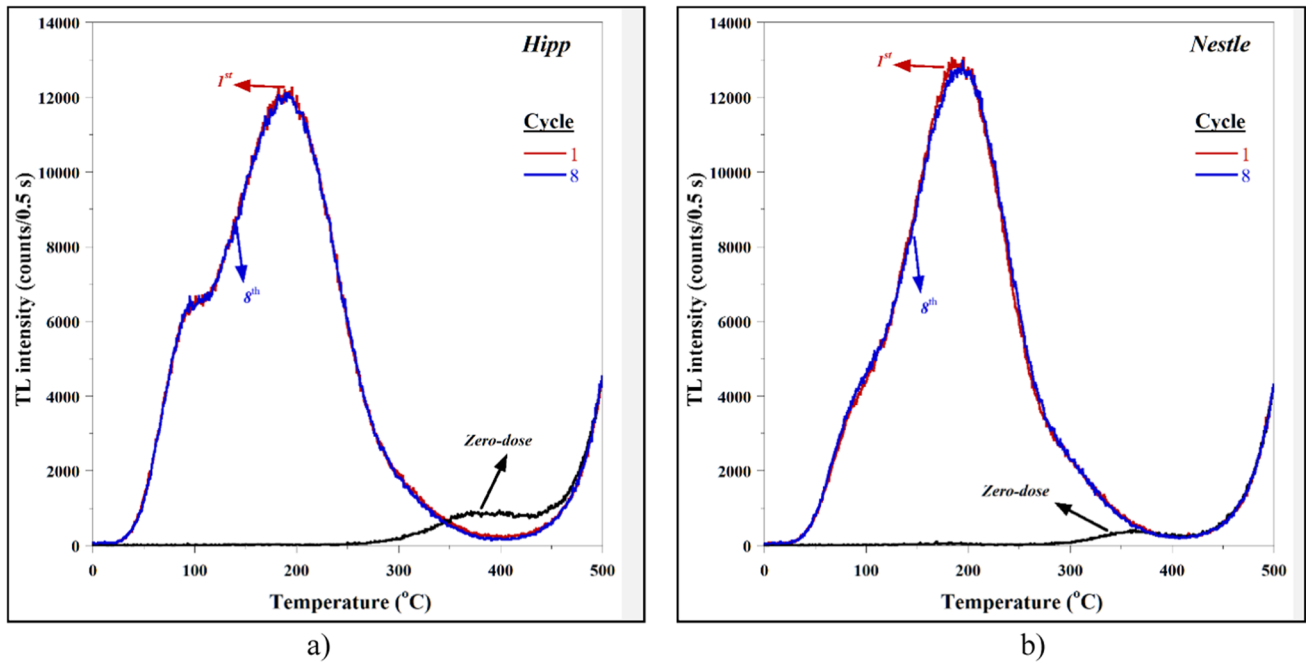
1534

Eur. Phys. J. Spec. Top. (2023) 232:1531–1542

Fig. 3 TL glow curves after consecutive dose/TL cycles for both glass containers: **a** Hipp and **b** Nestle

3.2 Sensitization of TL glow curve

To investigate the potential sensitization of the TL glow curve, a single aliquot of each glass container was subjected to eight consecutive cycles of irradiation and subsequent TL measurement, after the zero-dose response was acquired:

Step 1: TL (up to 500 °C) (zero-dose response).
  Step 2: Irradiation with test dose (50 Gy).
  Step 3: TL (up to 500 °C).
  Step 4: Repeat Steps 2 and 3 for seven more times.

Figure 3 illustrates the acquired glow curves only of the 1st and 8th cycles (for the sake of clarity) for both glass containers studied. It is obvious that no sensitization is observed for both containers since the consecutive irradiation-TL cycles do not affect the shape or the intensity of the peaks. The above is better illustrated in Fig. 4, where the normalized response in terms of total counts integrated in a specific temperature range for the various cycles is shown.

Counts were integrated in the temperature range 150–250 °C to avoid interference with the zero-dose signal and normalized to the integrated counts of the first cycle. The background was evaluated based on the zero dose TL signal and was subtracted from all data.

The response remains stable after the repeatable measurements (variation is less than 2%). The sensitization test was also conducted for a higher test dose (350 Gy) on a different aliquot as well to investigate if the sensitization is dose dependent. Results (not shown here) were similar indicating that single aliquot measurements are possible.
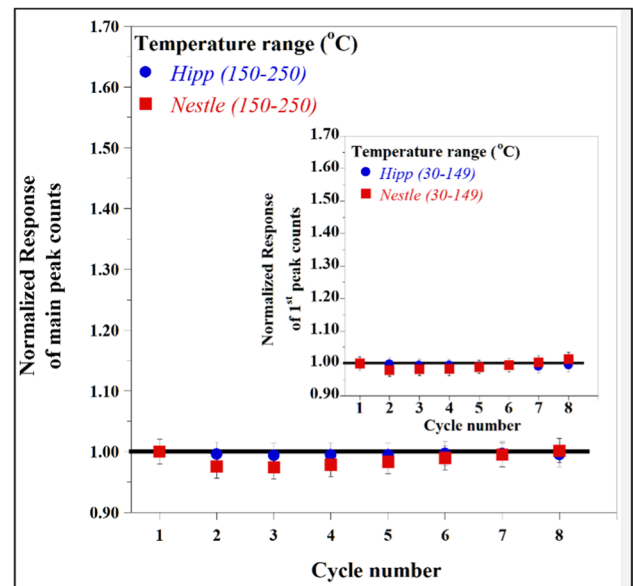

Fig. 4 Normalized TL response (temperature range 150–250 °C) for both glass containers after consecutive dose/TL cycles. The insets illustrate the normalized response for the lower temperature range (30–149 °C); error bars are at 2%

3.3 Dose response

The protocol followed, considered the investigation of the TL dose response in a single aliquot for both Hipp and Nestle. More specifically, the protocol consisted of the following steps:
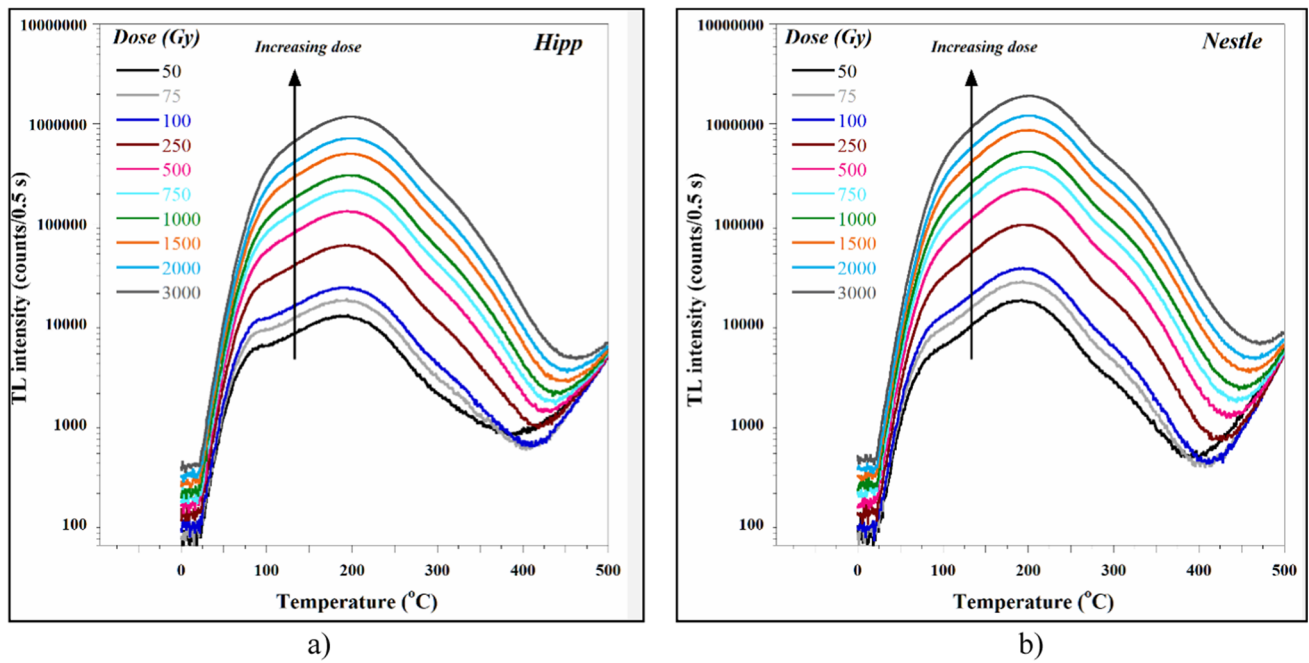
Eur. Phys. J. Spec. Top. (2023) 232:1531–1542

1535

Fig. 5 TL glow curves (semi-log scale) for various beta-doses: **a** Hipp and **b** Nestle
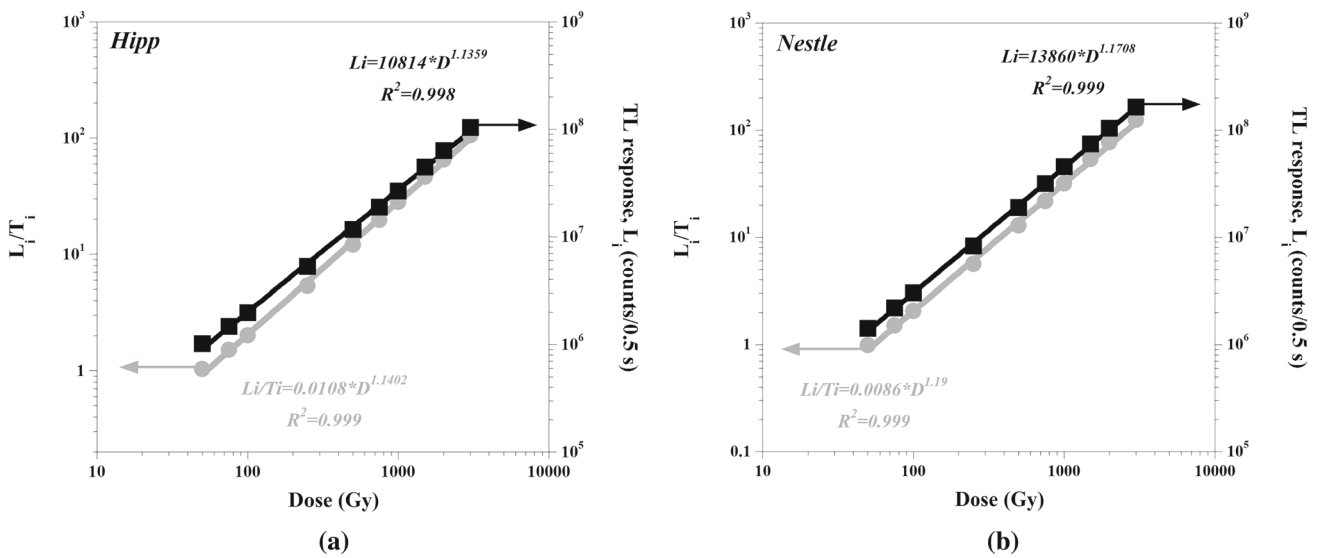

Fig. 6 Dose response (log–log scale) for the curve area counts corresponding to the temperature range 150–250 °C: **a** Hipp and **b** Nestle; the solid lines represent the regression lines derived from the equation given in the charts (of the form $Y = a*D^k$)

Step 1: TL (up to 500 °C) (zero-dose response).
 Step 2: Irradiation with dose i.
 Step 3: TL (up to 500 °C) (L_i response).
 Step 4: Irradiation with test dose (50 Gy).
 Step 5: TL (up to 500 °C) (T_i response).
 Step 6: Back to Step 2 with next dose i (where i =
50, 75, 100, 250, 500, 750, 1000, 1500, 2000, 3000 Gy).

Figure 5 illustrates the glow curves for various doses applied for both Hipp and Nestle. In both cases, as the dose is increased the second peak becomes wider and after a certain dose it begins to merge with the first

peak. Moreover, it is evident that no saturation has been reached up to a dose of 3 kGy, which is extremely important to use the containers as post-sterilization dosimeters of baby food.

Figure 6 depicts, in a log–log scale, the dose response for the curve area corresponding to the temperature range 150–250 °C. Response was calculated with two ways; considering only the L_i response (Step 3 from the above protocol) and calculating the ratio L_i/T_i (Step 3 and 5 respectively) as commonly performed for sensitization correction for dosimetry purposes. The available data were fitted with an equation of the form $Y =$

Table 1 Mathematical linear functions calculated from curve fitting for the L_i response (temperature range 150–250 °C) over the dose range 50–3000 Gy for both containers

Glass container	Function (Y = n + m·D)
Hipp	n = − 3.86 × 10^6 m = 34,498 (R^2 = 0.994)
Nestle	n = − 5.51 × 10^6 m = 55,323 (R^2 = 0.996)

$a*D^k$, where Y is the intensity L_i or the ratio L_i/T_i, D is the dose and a and k are constants (linear function in log–log scale). The value of the k is indicative of the linear behaviour of the material, namely if $k > 1$, supralinearity is observed, while if $k < 1$ a sublinear behaviour is evident [15].

In all cases, the value of k is close to unity indicating that dose response (temperature range 150–250 °C) is linear over the entire dose range studied (50–3000 Gy) for both glass containers and can be approximated with a linear fitting (Table 1). In addition, Fig. 6 verifies the previous findings that no sensitization of the materials is observed since results are similar considering either the L_i response or the L_i/T_i ratio.

3.4 Fading study

The stability of the TL signal under dark conditions storage was also investigated for various time periods (from 12 h up to 1 month). A test dose of 500 Gy was applied to various aliquots and the TL signal was recorded immediately after the irradiation. Then the same dose of 500 Gy was administered to the aliquots, and they were subsequently stored at room temperature in dark for various time periods. Then the TL of the corresponding aliquots was acquired after the corresponding storage time. The results of the fading study are illustrated in Fig. 7.

Both containers exhibit strong fading even after the first 12 h of storage over the entire temperature region even for the high temperature region, namely 150–300 °C.

The TL response was also calculated for the range 150–300 °C and was then normalized with the one acquired immediately after the initial irradiation (Fig. 8). After 7 days of storage the signal at the above region of interest (150–300 °C) fades almost 55% and 45% for Hipp and Nestle, respectively. For longer storage time the fading rate reduces, and the signal loss tends to remain constant. The experimental normalized TL data of the fading study can be explained best by a second order kinetic decay function [16]:

$$I_f = I_\infty + \frac{I_o'}{I_o' f t + 1}, \tag{1}$$

where $(I_\infty + I_o')$, I_f and I_∞ represent the normalized response at zero, any time and at infinity, respectively, while f and t represent the decay constant and the storage time, respectively. All calculated parameter values from the fitting procedure of the normalized data of the fading study are presented in Table 2. Obviously,
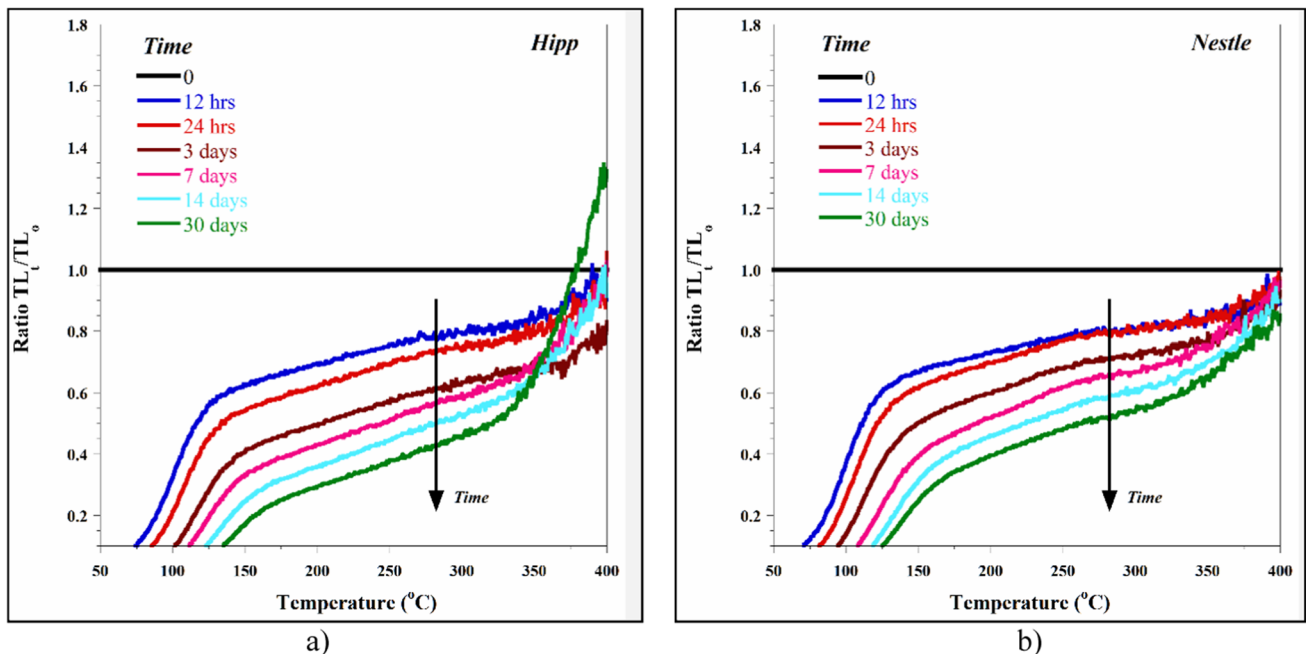

Fig. 7 Fading study for both containers: **a** Hipp and **b** Nestle. Figure shows the ratio of the glow curves for various storage periods after irradiation (500 Gy) with the one acquired directly after irradiation
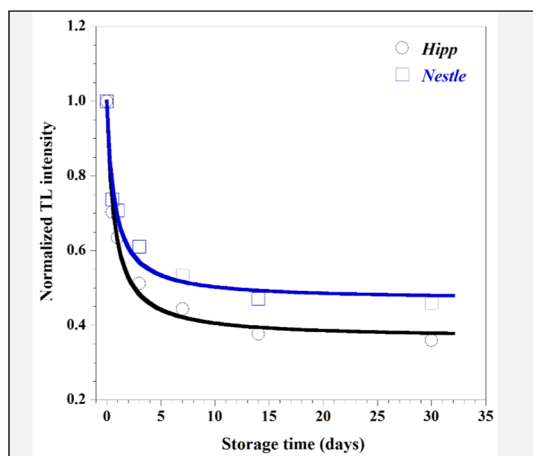
Fig. 8 Fading of the TL response for both containers for the main dosimetric peak area (150–300 °C) and their fitting (thick lines) with Eq. 1

Table 2 Values of the parameters of Eq. 1 for the area 150–300 °C calculated from the fitting procedure of the normalized data of the TL fading study for both containers

Baby food	I_∞	I_o'	f (days^{-1})	R^2
Hipp	0.365	0.635	2.272	0.999
Nestle	0.467	0.533	2.617	0.998

using Eq. 1 and the values of Table 2, one can directly calculate the fading factor for any storage time post irradiation for the area 150–300 °C for both containers.

3.5 Dose recovery test

A dose recovery test was also conducted to investigate whether an unknown exposure dose (e.g. sterilization) can be successfully calculated. For this purpose, the samples (two of each container) were first irradiated with an "unknown" nominal dose. The TL signal was recorded and then a dose response test was conducted on the same samples to acquire the calibration curve (counts of the 150–250 °C area were used for the integration). Linear regression was applied to the calibration data and the "unknown" dose was recovered by using the fitting curve. The nominal dose tested was 500 Gy. Table 3 presents the results of the recovery test, which indicate that the dose can successfully be recovered using the response of the area 150–250 °C. Figure 9 illustrates an example of the dose recovery test for one sample of each container.

3.6 TL Computerized curve deconvolution analysis (CCDA)

A computerized curve deconvolution analysis (CCDA) of the glow curves was also conducted for the various

Table 3 Comparison of nominal and recovered dose

Baby food	Nominal dose (Gy)	Recovered dose (Gy)	Difference (%)
Hipp-1	500	482.6	3.5
Hipp-2	500	489.0	2.2
Nestle-1	500	467.5	6.5
Nestle-2	500	468.7	6.3

doses for both Hipp and Nestle containers. Based on the material of the containers (glass) and the shape of the glow curves a similar approach with Kazakis [17] was adopted, namely considering that both discrete energy traps and continuous trapping states exist.

In the case of discrete energy traps, each peak can be fitted using a Levenberg–Marquardt algorithm with the analytical expression of the general order kinetics equation for TL developed by Kitis et al. [18]:

$$I(T) = I_m \cdot b^{\frac{b}{b-1}} \cdot exp\left(\frac{E}{kT} \cdot \frac{T - T_m}{T_m}\right)$$

$$\cdot \left[(b-1) \cdot (1-\Delta) \cdot \frac{T^2}{T_m^2} \cdot exp\left(\frac{E}{kT} \cdot \frac{T - T_m}{T_m}\right) + Z_m\right]^{-\frac{b}{b-1}}$$

$$(2)$$

where T (K) is the temperature, I_m (a.u.) the intensity at the peak maximum, b the order of kinetics, E (eV) the activation energy, T_m (K) the position of the peak maximum, k the Boltzmann constant, $\Delta = 2kT/E$, $\Delta_m = 2kT_m/E$ and $Z_m = 1 + (b-1)\Delta_m$. The fitting parameters are therefore I_m, T_m, E and b.

Moreover, the values of the pre-exponential factor and the lifetime of the traps (at 25 °C) can also be calculated by the following equations using the mean values of the calculated kinetic parameters.

$$s = \frac{\beta E}{kT_m^2} \cdot \frac{1}{Z_m} exp\left(\frac{E}{kT_m}\right) \quad (3)$$

$$\tau = \left[s \cdot exp\left(-\frac{E}{kT}\right)\right]^{-1} \quad (4)$$

where β (K s^{-1}) is the heating rate, s (s^{-1}) is the pre-exponential factor and τ (s) is the trap lifetime at 25 °C, in the case of discrete energy traps using general order kinetics.

On the other hand, Hornyak and Chen [19] gave an expression to describe the TL of materials with continuous distribution of trapping states uniformly distributed over a finite energy range $\Delta E = E_2 - E_1$, assuming first order kinetics. Later, Kitis and Gomez-Ros [20] formulated an algorithm for the decomposition of such glow-curves into its individual glow-peaks using only four experimental parameters. The correct formulation of the suggested algorithm for the case of such traps is [20, 21]:
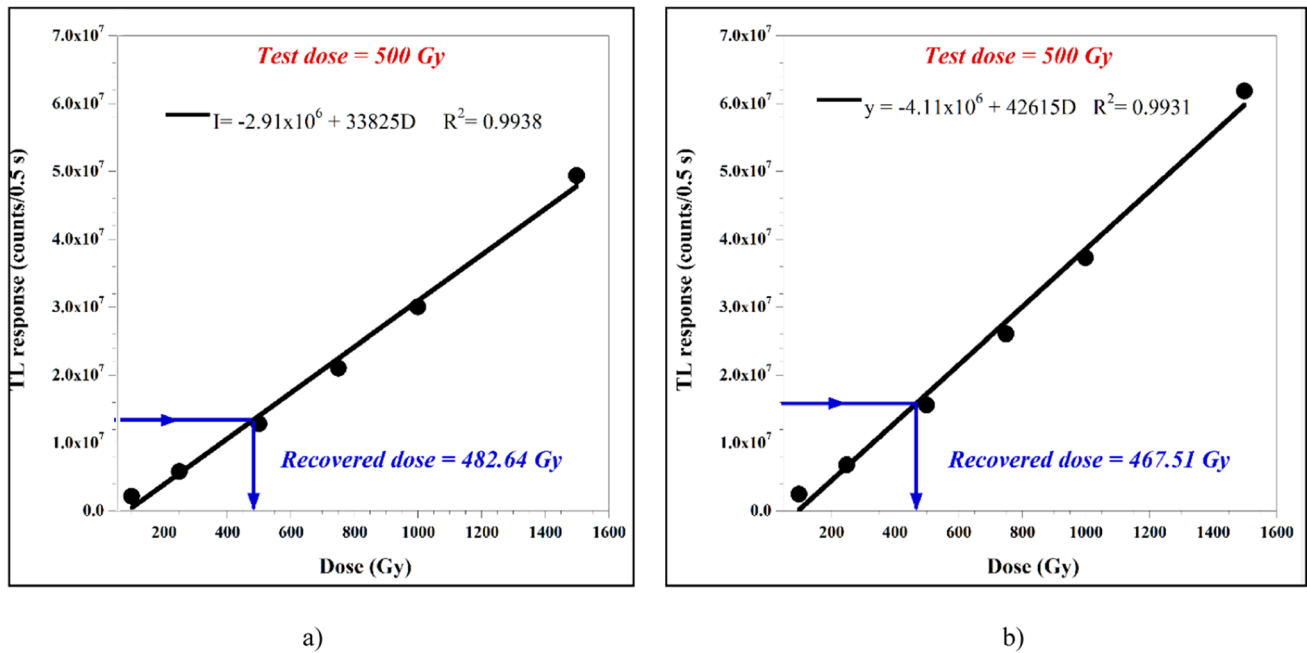
Fig. 9 Example of dose recovery test: **a** Hipp and **b** Nestle. The black circles represent the calibration data and the solid line their linear fitting

$$I(T) = I_m \frac{T_m}{T} \cdot \frac{1 - \Delta_m}{1 - \Delta} \cdot \frac{exp\left[-\frac{T^2}{T_m^2} \cdot (1 - \Delta) \cdot exp(u_{eff}) \cdot exp(-w)\right] - exp\left[-\frac{T^2}{T_m^2} \cdot (1 - \Delta) \cdot exp(u_{eff}) \cdot exp(w)\right]}{exp[-(1 - \Delta_m) \cdot exp(-w_m)] - exp[-(1 - \Delta_m) \cdot exp(w_m)]}$$

(5)

where E_{eff} (eV) is the effective activation energy defined as $E_{eff} = (E_2 + E_1)/2$, $w = \Delta E/2kT$, $w_m = \Delta E/2kT_m$ and $u_{eff} = E_{eff}(T - T_m)/kTT_m$. The rest of the parameters are the same as previously defined; only now E_{eff} is used instead of E.

Thus, the TL emission of a semi-crystalline substance or a material with intermediate defect population can be described by a superposition of Eqs. 2 and 5, considering that traps of various energy states exist, namely of discrete energy and continuous distribution. The CCDA was accomplished using the "TLDecoxcel" excel spreadsheet [22] which is designed to deconvolute glow curves with such an approach.

Glow curves of a dose range 50–3000 Gy were analyzed to individual components following the criteria described in [17], namely:

a. the smallest number of individual curves (components), sufficient to fit the experimental data, was used,
b. the kinetic parameters of each component must be similar within an acceptable error for all the curves for the doses in the studied range,
c. the integrated area of each component should keep a very clear functional relationship with the dose,

d. the sum of the integrated area of all components should exhibit a similar functional relationship with the dose to that of the experimental curve.

The goodness of the fit was tested using the well-known figure of merit (F.O.M) [23], which in its general form is:

$$F.O.M.(\%) = 100 \cdot \sum_{c=1}^{n} \frac{|Curve_{exp} - Curve_{fit}|_c}{A_{fit}}$$

(6)

where n is the total number of channels, $Curve_{exp_c}$ is the counts of the experimental glow curve in channel c, $Curve_{fit_c}$ is the summation of the counts of all p individual glow curves in channel c (i.e., $Curve_{fit_c} = \sum_{i=1}^{p} Y_{fit_{c_i}}$, where Y_{fit_c} is the counts of each individual glow curve in channel c) and A_{fit} is the total integration of all individual glow curves and channels (i.e., $A_{fit} = \sum_{c=1}^{n} Curve_{fit_c}$).

All results of the CCDA match very well the above criteria and the obtained F.O.M. was below 2.3%. Figure 10 presents an example of the fitting using both
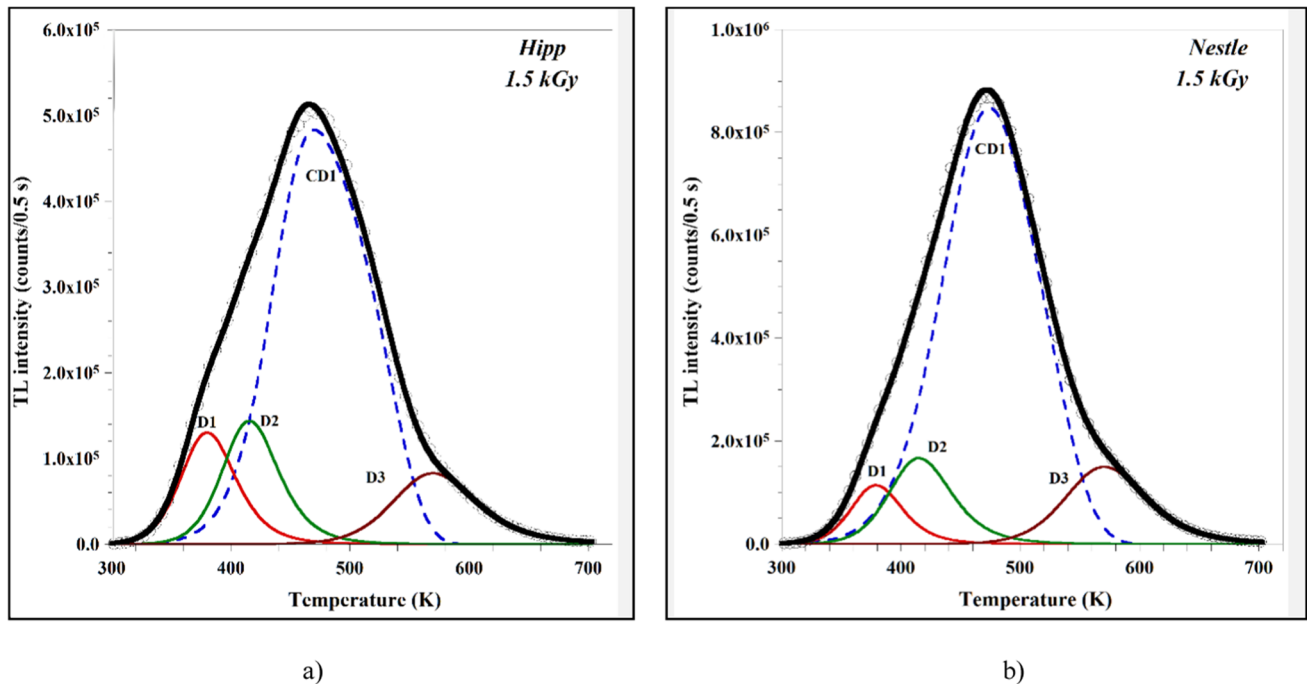
a)

b)

Fig. 10 Examples of the CCDA of the TL glow curves considering both discrete energy traps and continuous trap distribution for: **a** Hipp and **b** Nestle; experimental data (open circles) refer to those after exposure to 1.5 kGy; the thick line is the sum of all calculated components using Eq. 2 (discrete energy traps-solid lines) and Eq. 5 (continuous trap distribution-dotted lines) and the background; "D" stands for discrete energy traps and "CD" for continuous trap distribution

Table 4 Average values of the kinetic parameters of the components obtained by CCDA for Hipp

Peak	T_m (K)	E or E_{eff} (eV)	ΔE (eV)	b	s (s^{-1})	τ (years)
D1	372 ± 9	0.73 ± 0.02	–	2.00 ± 0.00	1.02×10^9	7.93×10^{-5}
D2	411 ± 5	0.90 ± 0.04	–	2.00 ± 0.00	1.30×10^{10}	3.84×10^{-3}
D3	567 ± 3	1.08 ± 0.07	–	2.00 ± 0.00	2.71×10^8	1.90×10^2
CD1	483 ± 3	0.78 ± 0.02	0.17 ± 0.01	–	–	–

discrete energy traps and continuous trapping states for the dose of the 1.5 kGy for both containers. Three (3) discrete-energy peaks D1, D2 and D3 and one (1) peak of continuous distribution traps were required to give a high-quality fit for both.

The resulting values of the kinetic parameters of the continuous-trap-distribution components used for the TL deconvolution are presented in Tables 4 and 5 for Hipp and Nestle, respectively. Results show that, in fact, the CCDA of all glow curves was achieved with almost the same values of the kinetic parameters. The value of each parameter is the mean of the values obtained from the glow curves of all doses. The CCDA shows that the components have similar kinetic parameters in both containers with negligible differences, which is an indication that they are probably manufactured by similar materials.

Based on the CCDA results, it seems that peak D3 has a long lifetime at both glass containers which could be employed for post-sterilization dosimetry purposes in baby-foods. For such purposes, a TL signal stable for an adequate period (from the sterilization up to the

expiration date) is required. To this respect, the faded glow curves were deconvoluted for all storage time periods, using the peaks (components) and the same kinetic parameters as previously found (Tables 4, 5). The only parameter allowed to vary during the CCDA was their maximum intensity I_m. An example of the CCDA on the faded curve for the case of seven (7) days after the irradiation is given in Fig. 11 for both glass containers.

From Fig. 11 it is obvious that the shape of the glow curve (typical for all storage times) changes at the low-temperature part, since it starts to rise at higher temperature. The CCDA of the faded glow curves showed that the shallow-trap peaks fade either completely (D1) or to a certain degree (D2 and the low-temperature part of the CD1). As expected, based on Tables 4 and 5, D3 exhibits a more stable behavior, thus could be used for dosimetry purposes.

Additionally, the integrated area of the continuous distribution traps peak and the discrete-energy peaks resulting from the CCDA analysis have a very good functional dependence on dose for both glass containers. Figure 12 presents the dose response of peaks CD1

1540

Eur. Phys. J. Spec. Top. (2023) 232:1531–1542

Table 5 Average values of the kinetic parameters of the components obtained by CCDA for Nestle

Peak	T_m (K)	E or E_{eff} (eV)	ΔE (eV)	b	s (s^{-1})	τ (years)
D1	372 ± 8	0.74 ± 0.04	–	2.00 ± 0.00	1.13×10^9	8.61×10^{-5}
D2	411 ± 3	0.79 ± 0.08	–	2.00 ± 0.00	4.85×10^8	1.52×10^{-3}
D3	567 ± 5	1.16 ± 0.07	–	2.00 ± 0.00	1.55×10^9	8.04×10^2
CD1	482 ± 2	0.66 ± 0.05	0.13 ± 0.01	–	–	–
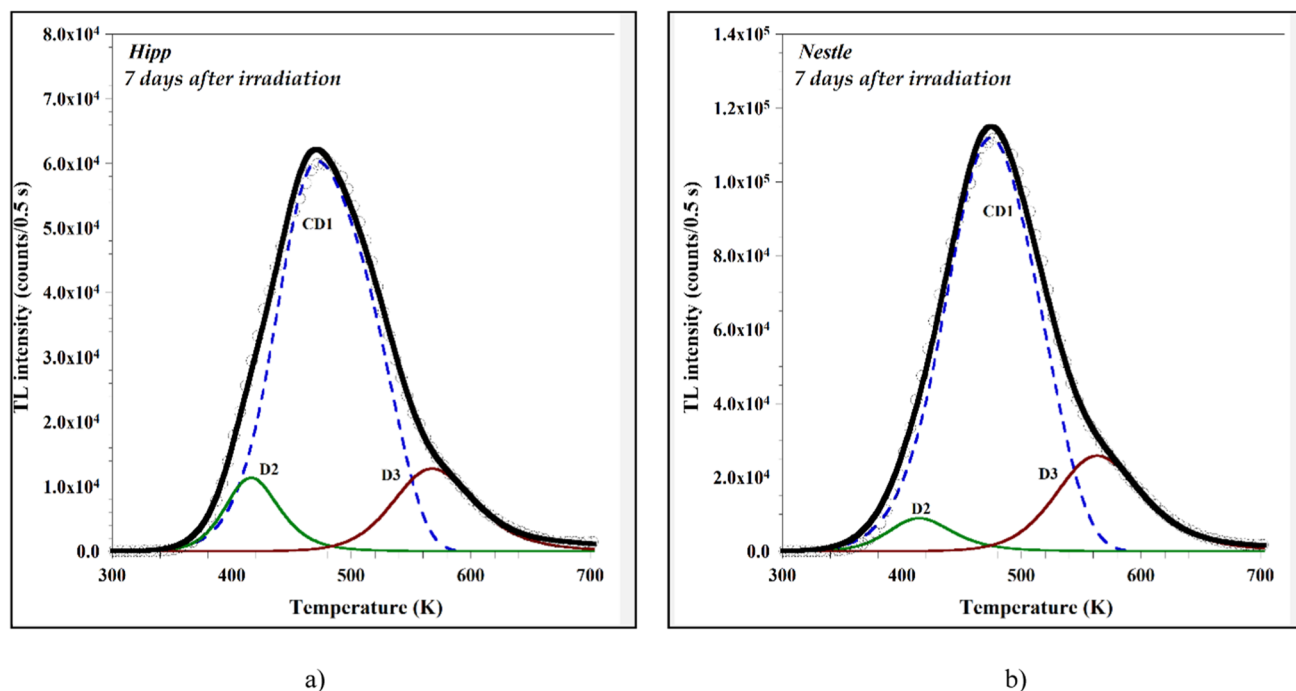
Fig. 11 Deconvolution of the faded signal 7 days after irradiation in the case of **a** Hipp and **b** Nestle; open circles are the experimental data, while the thick line is the sum of all calculated components using Eq. 2 (discrete energy traps-solid lines) and Eq. 5 (continuous trap distribution-dotted lines) and the background

and D3 for both glass containers. In both cases, data of peaks D1 and D2 are not presented due to their overlapping with data of component D3. However, a similar power function can also describe the respective behaviour of these peaks for the dose range 50–3000 Gy.

A linear function for the TL dose response could also be considered for all individual components of both glass containers, as given in Table 6, which could be used for post-sterilization dosimetry purposes.

4 Conclusions

The present work presents data regarding the luminescence properties of glass containers of two widely known baby foods to explore their efficiency as dosimeters for the detection of irradiated baby food.

Results indicate that the glow curves of both containers are similar, and they are composed by at least three peaks, which cannot be easily distinguished, since they are highly overlapping. Both baby-food containers

do not exhibit any sensitization allowing the repeatable use of the same aliquot for any measurement. It is evident that no saturation has been reached up to a dose of 3 kGy, which is extremely vital for their use as post-sterilization dosimeters of baby food.

In addition, a linear dose response is evident in the entire dose range studied (50–3000 Gy), while the use of the containers as dosimetric probes is validated by conducting dose recovery tests. It is shown that the delivered dose (500 Gy) is retrieved with high accuracy.

Both containers exhibit strong fading, thus fading correction is needed for their use as post-sterilization dosimeters. However, the respective fading factor for various storage periods can be calculated by fitting the experimental normalized TL data with a second order kinetic decay function for the various peaks.

The CCDA of the glow curves has been successfully conducted considering that both discrete energy traps and continuous trapping states exist. Results of the CCDA showed that they are composed by at least one peak of continuous trap distribution and three
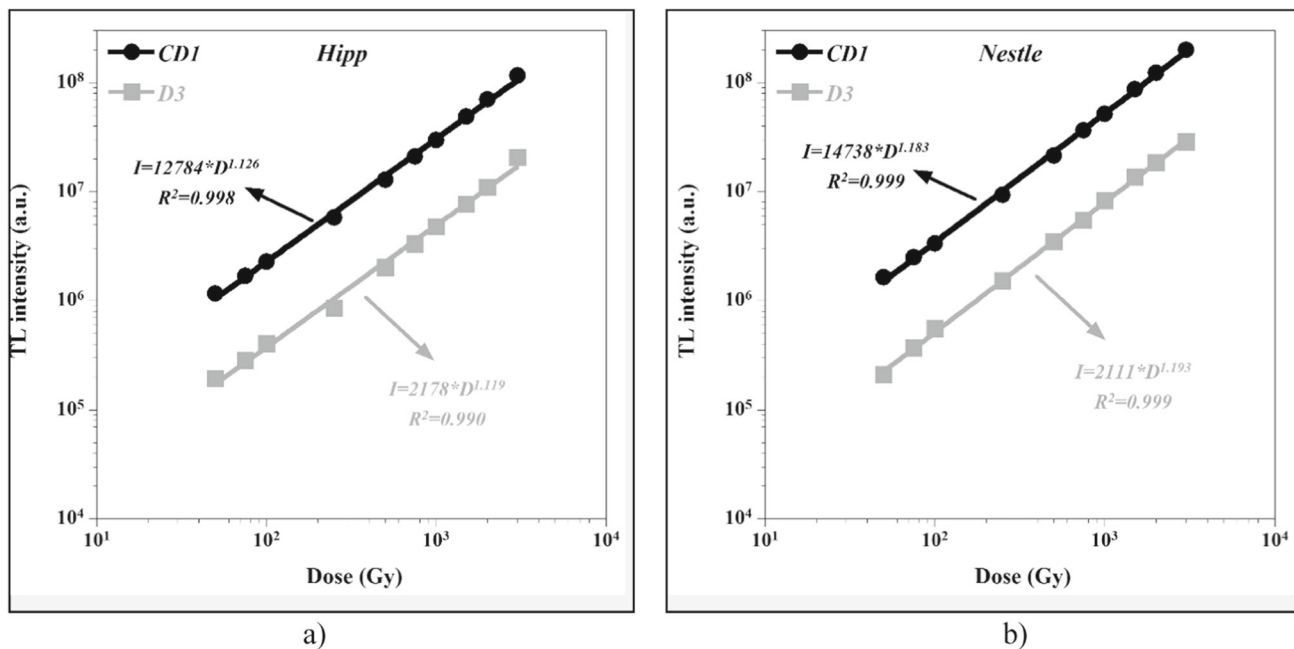
Fig. 12 TL dose response (log–log scale) of the components resulting from the CCDA for: **a** Hipp and **b** Nestle; the solid lines represent the regression lines of the form $Y = a*D^k$

Table 6 Mathematical linear functions calculated from curve fitting for the TL response of the continuous distribution traps and the discrete energy peaks found from the CCDA for both containers (dose range 50–3000 Gy)

Glass container	Peak	Function ($I = x + y \cdot D$)
Hipp	D1	$x = -245,449$ $y = 5684.6$ ($R^2 = 0.997$)
	D2	$x = -397,327$ $y = 6345.3$ ($R^2 = 0.998$)
	D3	$x = -963,014$ $y = 6586.7$ ($R^2 = 0.998$)
	CD1	$x = -4.28 \times 10^6$ $y = 38,084.3$ ($R^2 = 0.990$)
Nestle	D1	$x = -22,379$ $y = 4341.8$ ($R^2 = 0.999$)
	D2	$x = -106,348$ $y = 7631.4$ ($R^2 = 0.998$)
	D3	$x = -865,439$ $y = 9653.2$ ($R^2 = 0.997$)
	CD1	$x = -7.71 \times 10^6$ $y = 66,367$ ($R^2 = 0.993$)

discrete-energy peaks, which also demonstrate a linear dose response. However, CCDA of the faded glow curves showed that the low-temperature peaks exhibit strong fading, thus only the high-temperature part of the continuous-trap-distribution peak (CD1) and the D3 discrete energy peak seem appropriate for dosimetry purposes.

The present findings are promising towards the use of glass containers for the identification of baby food sterilized with ionizing radiation since they would be equally and jointly exposed to the ionizing radiation during the sterilization process. Future work should be focused on baby-food containers of different material or on solid baby-food products after the extraction of the luminescent minerals.

Data availability statement The datasets generated during and/or analysed during the current study are available from the corresponding author on reasonable request.

1542

Eur. Phys. J. Spec. Top. (2023) 232:1531–1542

References

1. European Union, List of Approved facilities for the treatment of foods and food ingredients with ionizing radiation in the Member States. OJEU C **37**(62), 6 (2019)
2. European Union, List of Member States' authorizations of food and food ingredients which may be treated with ionizing radiation. OJEU C **283**(52), 5 (2009)
3. Directive 1999/2/EC of the European Parliament and of the Council of 22 February 1999 on the approximation of the laws of the Member States concerning foods and food ingredients treated with ionising radiation, OJL **66**, 16 (1999).
4. National Cancer Institute (NCI) 2017. Antioxidants and cancer prevention. https://www.cancer.gov/about-cancer/causes-prevention/risk/diet/antioxidants-fact-sheet.
5. C.R. Harrell, V. Djonov, C. Fellabaum, V. Volarevic, Risks of using sterilization by gamma radiation: the other side of the coin. Int. J. Med. Sci. **15**(3), 274–279 (2018)
6. R.S.M. Frohnsdorff, Sterilization of medical products in Europe. Radiat. Phys. Chem. **17**(2), 95–106 (1981)
7. I.S. Arvanitoyannis, *Irradiation of food commodities: techniques, applications, detection, legislation, safety and consumer opinion* (Academic Press, London, 2010)
8. Food and Agriculture Organization of the United Nations and the World Health Organization, Standard for canned baby food, CODEX ALIMENTARIUS, International Food Standards, CXS 73-1981.
9. National Research Council (US) Committee on Pesticides in the Diets of Infants and Children. Pesticides in the Diets of Infants and Children. Washington (DC): National Academies Press (US) (1993).
10. J.V. Woodside, Nutritional aspects of irradiated food. Stewart Postharvest Rev. **3**, 2 (2015)
11. N.A. Kazakis, G. Kitis, N.C. Tsirliganis, Preliminary thermoluminescence investigation of commercial pharmaceutical glass containers towards the sterilization dosimetry of liquid drugs. Appl. Radiat. Isot. **105**, 130–138 (2015)

12. F.A. Balogun, F.O. Ogundare, M.K. Fasasi, TL response of sodalime glass at high doses. Nucl. Instrum. Methods Phys. Res. A **505**, 407–410 (2003)
13. A. El-Adawy, N.E. Khaled, A.R. El-Sersy, A. Hussein, H. Donya, TL dosimetric properties of Li2O–B2O3 glasses for gamma dosimetry. Appl. Radiat. Isot. **68**(6), 1132–1136 (2010)
14. B. Engin, C. Aydaş, H. Demirtaş, Study of the thermoluminescence dosimetric properties of window glass. Radiat. Effects Defects Solids Incorp. Plasma Sci. Plasma Tech. **165**(1), 54–64 (2010)
15. R. Chen, S.W.S. McKeever, *Theory of Thermoluminescence and Related Phenomena* (World Scientific Publishing Co. Pte. Ltd, Singapore, 1997)
16. C. Aydaş, Ü.R. Yüce, B. Engin, G. Polymeris, Dosimetric and kinetic characteristics of watch glass sample. Radiat. Meas. **85**, 78–87 (2016)
17. N.A. Kazakis, A detailed investigation of the TL and OSL trap properties and signal stability of commercial pharmaceutical glass containers towards their use as post-sterilization dosimeters of liquid drugs. J. Lumin. **196**, 347–358 (2018)
18. G. Kitis, J. Gomez-Ros, J. Tuyn, Thermoluminescence glow-curve deconvolution functions for first, second and general orders of kinetics. J. Phys. D Appl. Phys. **31**(19), 2636–2641 (1998)
19. W.F. Hornyak, R. Chen, Thermoluminescence and phosphorescence with a continuous distribution of activation energies. J. Lumin. **44**, 73–81 (1989)
20. G. Kitis, J.M. Gomez-Ros, Thermoluminescence glow-curve deconvolution functions for mixed order of kinetics and continuous trap distribution. Nucl. Instrum. Methods Phys. Res. A **440**, 224–231 (2000)
21. N.A. Kazakis, Comment on the paper "Thermoluminescence glow-curve deconvolution functions for mixed order of kinetics and continuous trap distribution by G. Kitis, J.M. Gomez-Ros, Nucl. Instrum. Methods Phys. Res. A 440, 2000, pp 224-231." Nucl. Instrum Methods Phys. Res. A **877**, 367–370 (2017)
22. N.A. Kazakis, TLDecoxcel: a dynamic excel spreadsheet for the computerised curve deconvolution of TL glow curves into discrete-energy and/or continuous-energy-distribution peaks. Radiat. Prot. Dosimetry **187**(2), 154–163 (2019)
23. H.G. Balian, N.W. Eddy, Figure-Of-Merit (FOM), An improved criterion over the normalized Chi-squared test for assessing goodness-of-fit of gamma–ray spectral peaks. Nucl. Instrum. Methods **145**(2), 389–395 (1977)